

Intermittency and fractal behaviour of charged particles generated using EPOS4 and PYTHIA8 at LHC energies

Fakhar Ul Haider,^{*} Ramni Gupta,[†] Salman Khurshid Malik,[‡] Balwan Singh,[§] and Zarina Banoo[¶]

Department of Physics, University of Jammu, Jammu, J&K, India

(Dated: May 26, 2026)

Large density fluctuations of charged particles are the promising signatures for exploring the QCD phase transition and critical point in heavy-ion collisions. These fluctuations are expected to exhibit fractal and scale-invariant behaviour, which is probed using intermittency methodology. Intermittency is the phenomenon of power-law growth of the normalized factorial moments ($F_q(M)$) of the number density distributions over decreasing bin size. This is studied for the charged particles simulated using PYTHIA8 and EPOS4 (UrQMD ON/OFF) for Pb–Pb collisions at $\sqrt{s_{NN}} = 5.02$ TeV. Scaling behaviour of $F_q(M)$ are studied as a function of phase space partitioning and second order moments to quantify the particle production nature within the default constraints of the two models. The scaling exponent related to the phase transition and parameters connected to fractal nature obtained for these models are also reported.

I. INTRODUCTION

The Quark Gluon Plasma (QGP) [1], a deconfined state of quarks and gluons is one of the most intriguing frontiers in high-energy physics. Believed to have existed a few microseconds after the Big Bang [2], the QGP offers a unique opportunity to study the fundamental dynamics of Quantum Chromodynamics (QCD) [3] under extreme conditions. QCD predicts that, at sufficiently high temperature and baryon density, strongly interacting matter undergoes a phase transition from hadronic matter to a deconfined state of matter (QGP) [4–6]. Mapping the QCD phase diagram and locating the critical point is one of the central goals in the field. Experiments at the Large Hadron Collider (LHC) [7] recreate these extreme conditions through ultra-relativistic heavy-ion collisions, producing a small short-lived but extremely hot and dense medium that rapidly expands, cools, and hadronizes. A large number of particles are produced during these collision experiments that provide valuable insight into the properties of QGP and that of strongly interacting matter under extreme conditions. Fluctuations in the number of these produced particles, called multiplicity fluctuations [8, 9], is one of the numerous observables which are used in the field to perform studies to get answers to many such unknown aspects of nature. Multiplicity fluctuations is a sensitive probe to the underlying particle production mechanism and the dynamics of the system involved [10, 11]. An understanding about the QCD phase transition can be developed by studying the

scaling behaviour of the normalized factorial moments of the number density distributions [12]. The power-law scaling behaviour of the NFM with the decreasing bin size, termed as intermittency, is a promising tool to investigate properties of dynamic systems. Studies on the ISING model [13, 14] have revealed that the intermittency [15] in QCD second order phase transition exhibits anomalous scaling behaviour and that gives the fractal dimension (d_q) is $1/8$, regardless of the moment order "q". Empirical evidence from heavy ion collisions and other interactions suggests multifractal behaviour [16, 17] of system. It is observed in Ginzburg-Landau (GL) theory that the anomalous fractal dimension is not constant and is related to the moment order through a universal scaling [18] that is applicable to all systems described by GL theory for second-order phase transitions. This universality is particularly significant for QCD phase transitions, where key parameters like transition temperature remain unknown. The LHC's unprecedented collision energies and large multiplicities provide a rich source of data that can be exploited to comprehend these phenomena in greater detail, offering the possibility of detecting new physics and refining available successful theoretical models of QCD.

This article presents intermittency and fractal nature study of the events generated using the PYTHIA8 [19] + Agantyr and EPOS4 [20] in two modes. Section II gives a brief overview of the MC event generators and event samples. The methodology of analysis is given in section III followed by observations and results in the section IV. Section V gives the summary of this study.

II. MONTE CARLO EVENT GENERATORS AND EVENTS SAMPLES

In high energy collision physics, an event refers to a single instance of a particle collision, characterized by

* fakharulhaider@gmail.com

† ramni.gupta@cern.ch

‡ salmankm@keemail.me

§ balwan.singh@cern.ch

¶ zarina.banoo@cern.ch

the complete set of outgoing particles and their measurable properties, such as energy, momentum, and electric charge. These events are simulated using the software tools called event generators which are modelled using theoretical framework and probabilistic rules. Event generators employ Monte Carlo methods to produce realistic and statistically representative outcomes to understand data and to refine theoretical predictions. **PYTHIA 8** a general-purpose Monte Carlo event generator designed primarily for simulating high-energy proton–proton (pp) collisions is used. It provides a complete description of the event evolution, starting from the hard partonic scatterings to final-state hadron production. A key feature of PYTHIA 8 [19] is its detailed treatment of QCD parton scatterings through an extensive set of internally implemented ($2 \rightarrow 1$) and ($2 \rightarrow 2$) hard processes, complemented by multi-parton interaction (MPI) modeling [21], where several independent QCD scatterings can occur within a single event. These scatterings are regulated using an energy-dependent transverse momentum cutoff to avoid divergences at low p_T . The probability for multiple interactions is determined based on parton distribution functions and an overlap function that depends on the impact parameter of the collision. Colour reconnection schemes [22] limit the number of independent colour strings, thereby preventing an overproduction of soft particles at large rapidities and shapes the rapidity profile of final state particles.

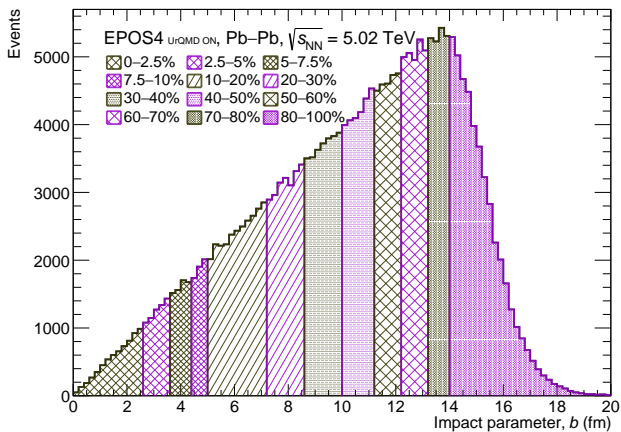


Figure 1: Impact-parameter distribution for Pb–Pb collisions at $\sqrt{s_{\text{NN}}} = 5.02$ TeV using EPOS4. Vertical boundaries in the plot indicates centrality percentiles.

To simulate more complex systems such as proton–nucleus (pA) and nucleus–nucleus (AA) collisions, the Angantyr [23] model extends PYTHIA 8 by embedding it within a Glauber-inspired [24] framework. In this approach, the number of binary nucleon–nucleon (NN)

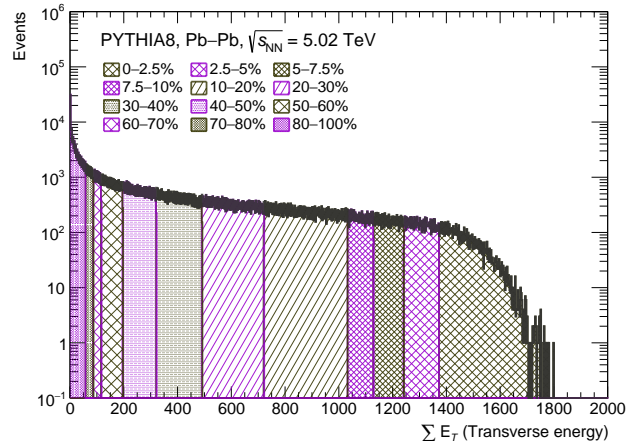


Figure 2: Distribution of the summed transverse energy, $\sum E_T$ used to define centrality classes for PYTHIA8 for Pb–Pb collisions at $\sqrt{s_{\text{NN}}} = 5.02$ TeV. Centrality intervals are shown by percentile boundaries.

sub-collisions is determined from the geometry of the collision using a Monte Carlo Glauber calculation [25].

In AA collisions, additional complexities such as energy–momentum conservation, impact parameter reweighting [26], and isospin adjustments are implemented to better reflect nuclear dynamics. Within this combined PYTHIA–Angantyr framework, multiplicity fluctuations originate from two main sources. First, geometric fluctuations that arise from variations in the number and configuration of NN sub-collisions from event-to-event. Second, internal fluctuations emerge from PYTHIA’s MPI model, which governs the number of partonic interactions within each NN sub-event. In pA and AA collisions [27, 28], these fluctuations are amplified due to the presence of secondary interactions and the varying energy available in the nucleon remnants. The interplay between these sources result in realistic multiplicity distributions and provides a reliable baseline for interpreting initial-state fluctuations, non-flow correlations and collective behaviour in heavy-ion collisions.

The second MC model that is studied is EPOS4 [29] model. EPOS4 is an event generator framework developed for simulating high-energy collisions like proton–proton (pp) and nucleus–nucleus (AA) interactions. It employs a rigorous parallel scattering framework that simultaneously models multiple parton–parton interactions within a single collision event, representing a significant advancement over traditional QCD-based event generators. This approach mitigates the limitations of conventional factorization schemes by enforcing exact energy–momentum conservation across all concur-

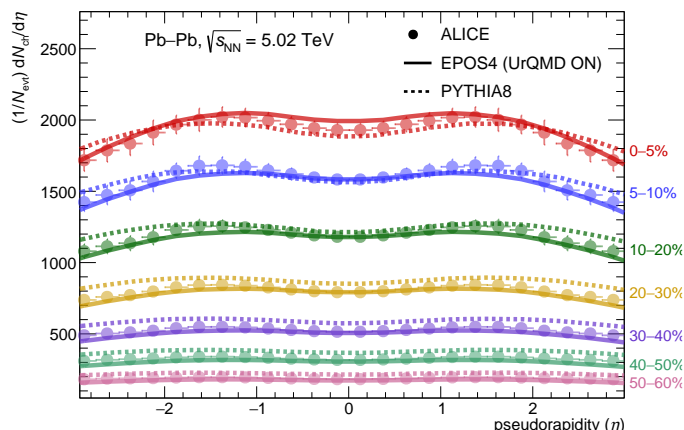


Figure 3: Charged-particle pseudorapidity density distributions normalized with number of events from Pb-Pb collisions at $\sqrt{s_{NN}} = 5.02$ TeV obtained using EPOS4 (solid lines) and PYTHIA8 (dotted lines) across various centralities are shown. The ALICE data (filled markers) [32] are also shown.

rent scattering processes [30]. This a treatment help to achieve a consistent and realistic description of the complex dynamics that govern high multiplicity collision events, where multiple interactions occur simultaneously and compete for the available energy.

Key strength of EPOS4 lies in its ability to compute dedicated parton distribution functions and inclusive cross sections, facilitating accurate descriptions of hard probes like jets in conjunction with the underlying soft background and global particle production. This allows for a unified description of observables ranging from jet spectra and particle ratios to flow harmonics and centrality-dependent distributions. It is capable of modelling charged-particle production for various collision systems and centrality classes, thereby providing a detailed understanding of the mechanisms governing particle generation, hadronization, and subsequent final-state dynamics [31].

Within EPOS4, particle production is organized through a core-corona separation, in which the system formed at early times is decomposed into regions of high and low density. The high-density component gives rise to a collectively expanding medium described by hydrodynamics, while particles originating from the low-density component escape largely unaffected and hadronize without collective behaviour. This scheme provides a natural interpolation between thermalized and non-thermalized particle production across different collision systems. In addition, EPOS4 allows the inclusion of late-stage hadronic interactions by cou-

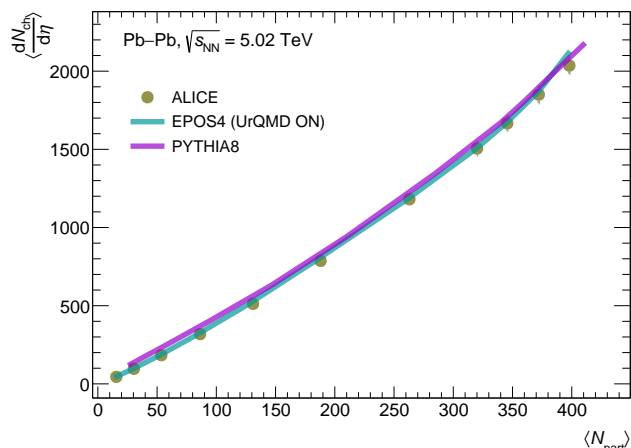


Figure 4: Mean charged particle density $\langle dN_{ch}/d\eta \rangle$ as a function of participant nucleons ($\langle N_{part} \rangle$) for EPOS4 mode and PYTHIA8, compared with ALICE measurements[33] for Pb-Pb at $\sqrt{s_{NN}} = 5.02$ TeV.

pling to the UrQMD transport model. Simulations with UrQMD enabled EPOS4 incorporate hadronic rescattering and resonance decays, whereas calculations without UrQMD effectively exclude the hadronic phase, offering a transparent way to quantify the influence of hadronic interactions on final-state observables [34].

Centrality determination characterizes the initial geometric overlap and event activity in heavy-ion collisions. Geometry proxies such as impact parameter (b), participant nucleons (N_{part}), and binary collisions (N_{coll}) in experiment are not directly measurable in an experiment and are typically inferred by correlating event activity (e.g., charged-particle yield or summed transverse energy) with a Glauber-based geometry [35]. In simulations, centrality can be defined either directly from the generated b or via midrapidity multiplicity/summed transverse energy within a chosen η window. Here centrality for the EPOS4 simulated events is determined using b where the distribution given in Figure 1 shows the number of events as a function of b . This distribution is divided into several percentiles based centrality classes corresponding to the most central to peripheral collisions. These intervals provide a systematic way to relate the geometric overlap of the colliding nuclei to event activity within the model.

For PYTHIA 8, centrality has been estimated using the distribution of the summed transverse energy ($\sum E_T$) in the final state. Figure 2 presents the $\sum E_T$ distribution, where the percentile boundaries defining the same centrality classes as used for EPOS4 (Fig. 1) are indicated. This approach allows a consistent comparison between EPOS4 and PYTHIA 8 by mapping the event activity in both models to a common central-

ity framework.

Figure 3 shows the normalized charged-particle pseudorapidity density distributions, $(1/N_{\text{evt}}) dN_{\text{ch}}/d\eta$, for different centrality classes, comparing EPOS4 (solid lines) and PYTHIA 8 (dotted lines) with ALICE experimental data (filled markers) [32] at $\sqrt{s_{\text{NN}}} = 5.02$ TeV. The results are presented for centrality intervals 0–5%, 5–10%, 10–20%, 20–30%, 30–40%, 40–50%, and 50–60%. Simulated events from the two models are observed to have generated tracks with η density very close to ALICE data in the mid-rapidity region. Figure 4 shows the mean charged-particle pseudorapidity density at midrapidity ($|\eta| < 0.8$) as a function of participant nucleons, for the events obtained from the two models. The ALICE data points are also shown. Model is observed to explain the mean charged particle pseudoeapidity density from the ALICE for Pb-Pb collisions at $\sqrt{s_{\text{NN}}} = 5.02$ TeV.

Figure 3 and 4 give a baseline characterization of the simulated events with regard to ALICE data and validate the consistency of event generation, the centrality determination of the events in the subsequent intermittency analysis.

III. METHODOLOGY

Intermittency analysis first introduced in 1986 [36] in the field of heavy ion collisions [37] has been used in various collision studies to reveal features of particle production. The methodology proposed for the study of scaling behaviour of charged particles generated as discussed above are studies for the scaling behaviour as discussed below.

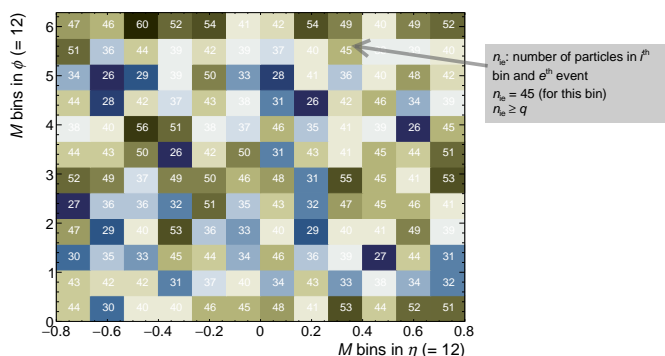


Figure 5: Schematic illustration of the two-dimensional phase-space partitioned into equal number of bins, (M) along η and in ϕ direction. The numbers inside the cells are for represent the particle counts n_{ie} termed as the bin multiplicity.

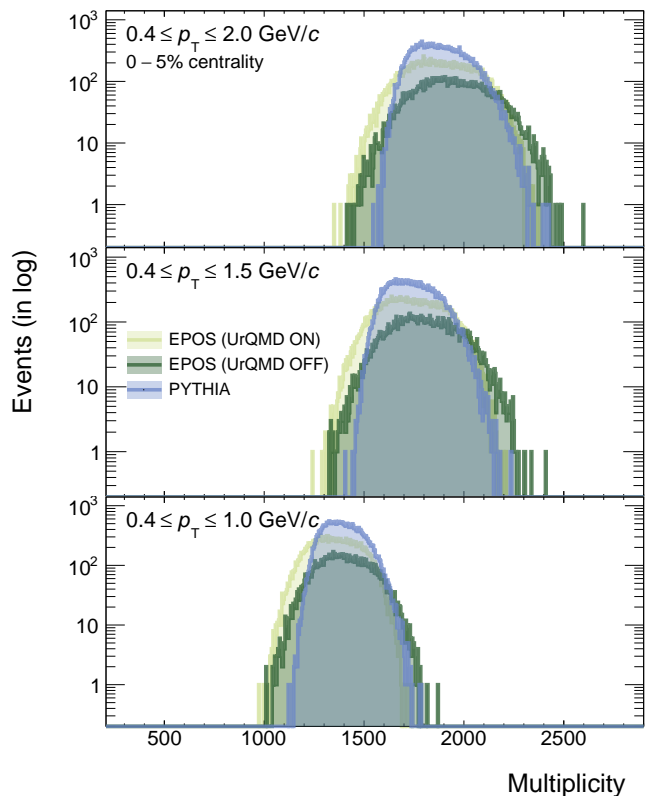


Figure 6: Charged-particle multiplicity distributions within $|\eta| \leq 0.8$ for 0–5% central events for the p_T ranges: $0.4 \leq p_T \leq 2.0$ (top), $0.4 \leq p_T \leq 1.5$ (middle), $0.4 \leq p_T \leq 1.0$ (bottom) shown on a logarithmic event count scale, obtained from Pb-Pb collisions at $\sqrt{s_{\text{NN}}} = 5.02$ TeV

The charged particles in two dimensional (η, ϕ) phase space of an event are distributed over the two dimensional (η, ϕ) grid, with $M(\eta)$ bins along the η axis and $M(\phi)$ bins along the ϕ axis, as shown in Figure 5. The normalized factorial moments of the particles in a bin (bin multiplicity) are determined to gain deeper insight into fluctuations in local density. The particle multiplicity moments characterize how particles are distributed within the phase space. The normalised factorial moments [36, 37] serve as a measure of departures from a Poissonian (random) distribution and are defined as:

$$F_q(M) = \frac{\frac{1}{N} \sum_{e=1}^N \frac{1}{M^2} \sum_{i=1}^M f_q^e(n_{ie})}{\left(\frac{1}{N} \sum_{e=1}^N \frac{1}{M^2} \sum_{i=1}^M f_1^e(n_{ie}) \right)^q} \quad (1)$$

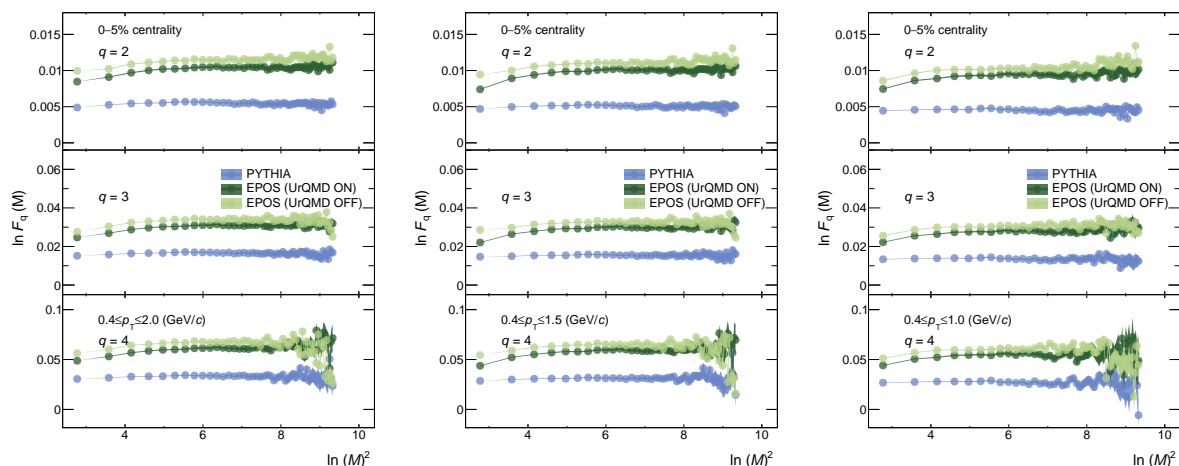


Figure 7: M-scaling of NFM: $\ln(F_q(M))$ as a function of $\ln M^2$ for 0–5% central events showing results and comparison of PYTHIA8, EPOS4 UrQMD ON and OFF modes for p_T ranges: $0.4 \leq p_T \leq 2.0$ (left), $0.4 \leq p_T \leq 1.5$ (middle), $0.4 \leq p_T \leq 1.0$ (right). Columns correspond to different orders of $F_q(M)$.

where,

$$f_q^e(n_{ie}) = \prod_{j=0}^{q-1} (n_{ie} - j) \quad (2)$$

Each bin in the grid with M^2 cells represents a specific region of the phase space, and n_{ie} indicates the number of particles in the i^{th} bin of the e^{th} event. For a system that exhibits dynamical fluctuations associated with critical behaviour, the normalized factorial moments $F_q(M)$ are expected to increase systematically as the number of phase-space partitions (M) grows giving linear dependence. This also reflects self-similar fluctuations and is commonly referred to as M-scaling, with the corresponding growth characterized by an intermittency index ϕ_q as

$$F_q(M) \propto M^{\phi_q}. \quad (3)$$

The parameter q is a positive integer greater than or equal to 2. A strict linear dependence of F_q on M is indicative of the presence of critical fluctuations and system being at critical point whereas on the other extreme a total independence is due to pure Poissonian nature of particle distribution. The scale invariant behaviour reflects the self-similar and fractal structures in the system. Fractals [38] are the structures with a fractional dimension exceeding their topological dimension, reflecting their inherent complexity and irregular geometry. Fractal dimensions and intermittency index are mathematically related as [39]:

$$D_q = D_T \left(1 - \frac{\phi_q}{q-1}\right) \quad (4)$$

D_q being independent of q suggests a monofractal system and multifractal system in case of any dependence. Fluctuations exhibit different scaling behaviours for different scales or regions [40] in case of multifractal system. In a statistically homogeneous fractal distribution [41], the properties of particle distributions remain invariant under scaling transformations, ensuring that the probability of detecting particles within a given volume is consistent across different regions of phase space. The power-law behaviour associated with a homogeneous fractal dimension then exhibits self-similarity across multiple scales. This fundamental property is subsequently reflected in the scale invariant behaviour of the NFM.

Further the order of the transition of a system from one phase to another, there can be different path ways. Order scaling is observed to be present in the systems going through second order phase transition such that

$$F_q(M) \propto (F_2(M))^{\beta_q}. \quad (5)$$

This power-law behaviour is referred to as F-scaling [18]. The exponent β_q characterizes the scaling behaviour of the higher-order factorial moments with respect to the second-order moment. It depends on factors such as the resolution of the bins. The power-law relationship between β_q and q , given by

$$\beta_q \propto (q-1)^\nu \quad (6)$$

This characterizes scaling behaviour across different moment orders and remains independent of the dimensionality of the phase space bins. ν is a dimensionless exponent.

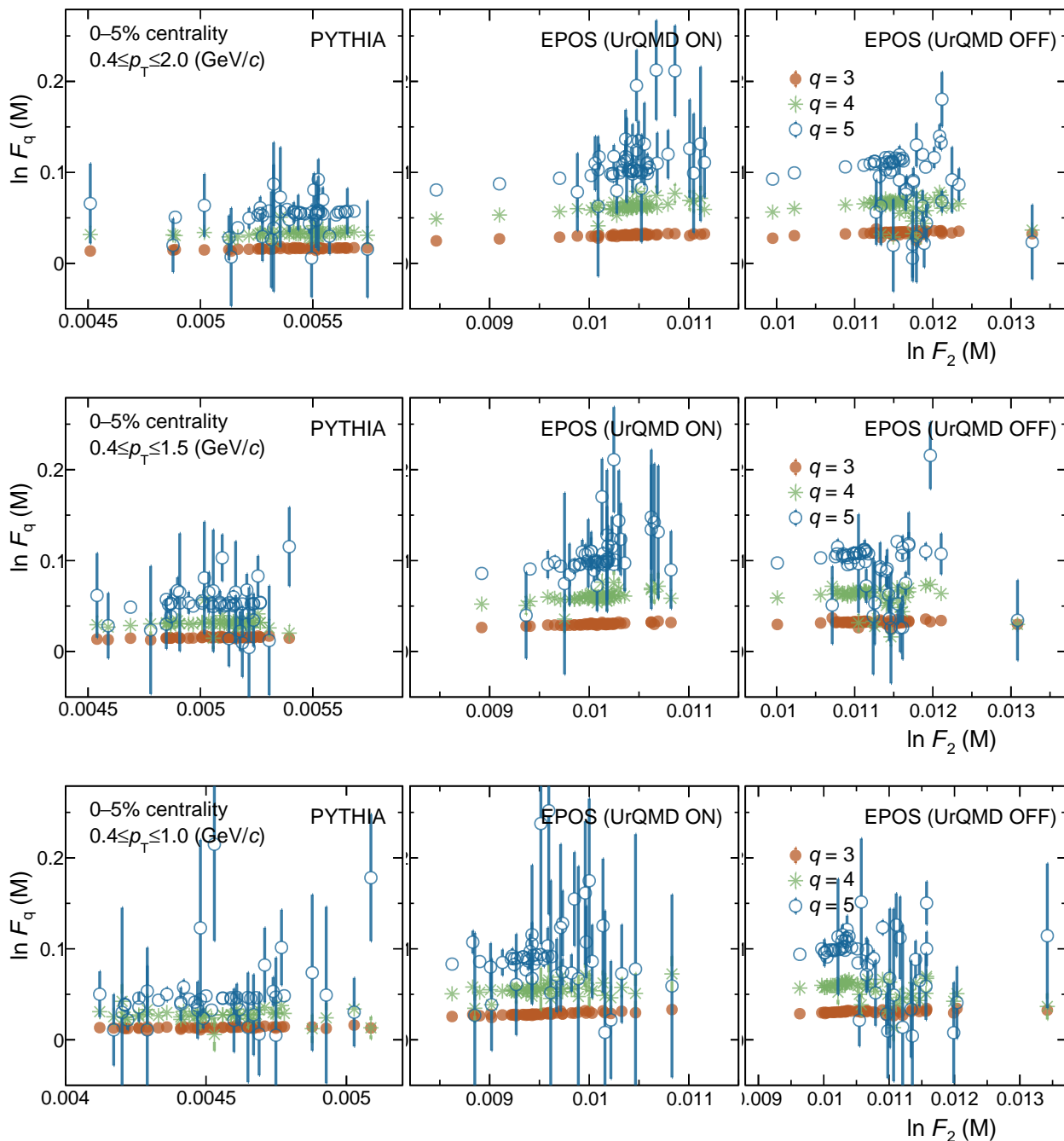


Figure 8: $\ln(F_q(M))$ as a function of $\ln(F_2(M))$ (F-scaling) for PYTHIA8, EPOS4 UrQMD ON and OFF modes for p_T ranges: $0.4 \leq p_T \leq 2.0$ (top), $0.4 \leq p_T \leq 1.5$ (middle), $0.4 \leq p_T \leq 1.0$ (bottom) for the most central 0-5% events.

IV. OBSERVATIONS AND RESULTS

A 200K PYTHIA8 and 300K EPOS4 events generated for Pb-Pb collisions at $\sqrt{s_{NN}} = 5.02$ TeV have

been analysed. The charged particles (π^\pm , K^\pm , p , \bar{p}) generated within the acceptance of $|\eta| \leq 0.8$, full azimuth ($0 \leq \phi \leq 2\pi$) are studied to look for scaling and fractal behaviour in the soft p_T intervals $0.4 \leq p_T \leq 2.0$, $0.4 \leq p_T \leq 1.5$, $0.4 \leq p_T \leq 1.0$ GeV/c. The multiplicity

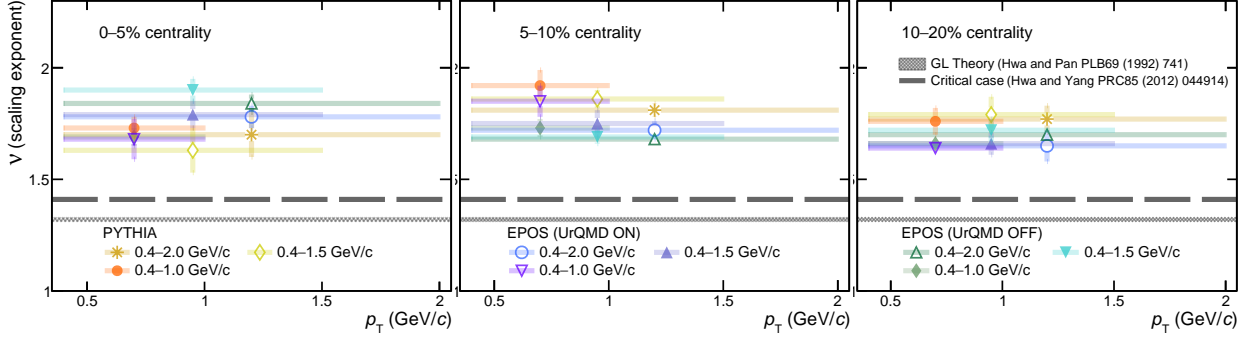


Figure 9: Scaling exponent, (ν) as a function of p_T for $0.4 \leq p_T \leq 2.0$, $0.4 \leq p_T \leq 1.5$, $0.4 \leq p_T \leq 1.0$ and 0–5% (left), 5–10% (middle), 10–20% (right) events.

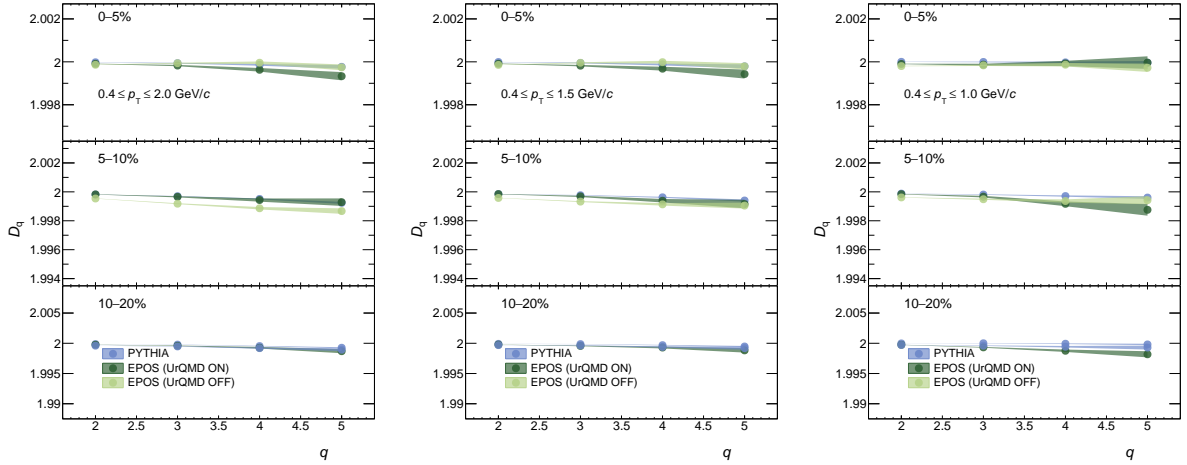


Figure 10: Generalized (Rényi) dimensions, D_q as a function of q for p_T ranges: $0.4 \leq p_T \leq 2.0$ (left), $0.4 \leq p_T \leq 1.5$ (middle), $0.4 \leq p_T \leq 1.0$ (right). Observations for charged particle generated events using PYTHIA8 and EPOS4 with UrQMD ON and OFF, in the centrality bins 0–5%, 5–10% and 10–20% events.

distributions of the charged particles within the kinematic bounds are shown in Fig. 6 for PYTHIA8 and two EPOS4 modes. The distributions are well described by Gaussian shapes with no secondary peaks.

$F_q(M)$ moments (Eq. 1) are calculated for $q = 2, 3, 4$ and 5. For this the number of bins (M) in (η, ϕ) phase space are taken for a minimum value of 4 to a maximum value of 82. For this the charged particles in an event are mapped onto the 2-dimensional (η, ϕ) grid for an M . After this the bin multiplicities and hence the factorial moment as defined in Eq. (2) are determined. This is repeated for all the events for each M and for each moment order $q = 2, 3, 4$ and 5. Normalized factorial moment (F_q) is then obtained from the event factorial moment. Figure 7 shows $F_q(M)$ variation with bin resolution of the phase space on a log-log plot for three p_T intervals ($0.4 \leq p_T \leq 2.0$ (left),

$0.4 \leq p_T \leq 1.5$ (middle), $0.4 \leq p_T \leq 1.0$ (right)); vertical bars denote statistical uncertainties obtained using sub-sampling method. It is observed that for $q \geq 2$, $F_{q+1}(M) \geq F_q(M)$ with an initial rise at small M followed by saturation. The initial rise is more pronounced for EPOS4 while PYTHIA8 shows no such behaviour. The independence of $F_q(M)$ on the increasing number of bins implying no robust M -scaling and therefore no intermittency. This shows that the particle generation process does not have scale-independent behaviour.

The intermittency indices ϕ_q are obtained as the slopes of the line fits in the high- M region of M -Scaling plots for $q = 2, 3, 4, 5$. They are used to determine the generalized (Rényi) dimensions D_q , with the phase-space dimensionality $D_T = 2$. Fig. 10 shows D_q vs q plots for the different p_T intervals studied. PYTHIA8 and EPOS4 model follow a similar trend

for all the centralities and p_T intervals. Within uncertainties (shown as colored bands), D_q exhibits negligible q -dependence, indicating a monofractal character of particle production and the absence of pronounced bin-to-bin density fluctuations in the analysed samples.

Figure 8 shows $\ln(F_q(M))$ as a function of $\ln(F_2(M))$ for $q = 3, 4$ and 5 . $\beta_3, \beta_4, \beta_5$ are determined from the linear fits to F-scaling plots, and using Eq. 6, scaling exponent (ν) is determined. ν as a function of p_T is shown in Fig. 9 for three centrality intervals: 0–5%, 5–10%, 10–20%. Horizontal bars denote the p_T range for each data point. GL theory [18] and SCR model [12] values in case of phase transformation also given that are far away from the values obtained with these two models. It is observed that ν from the three models across various centralities and p_T ranges is $1.6 \leq \nu \leq 1.9$. Values are larger than the predicted ones for in case the system is at criticality and presence of second order phase transition.

V. SUMMARY

The study presented above investigates the scaling behaviour of charged-particle multiplicity fluctuations in Pb–Pb collisions at $\sqrt{s_{NN}} = 5.02$ TeV using simulated event samples from the EPOS4 and PYTHIA 8 models. The analysis employs normalized factorial moments to explore local density fluctuations. Event samples generated with the EPOS4 model with hydrody-

namical and hydro+cascade configurations are compared with those from PYTHIA 8 to examine the sensitivity of intermittency observables to different underlying particle-production mechanisms.

The power-law M-scaling is observed to be absent for both models, as reflected by the absence of linear behavior in the $\ln F_q$ versus $\ln M$ plots. The extracted values of the scaling exponents are $\gg 1.3$ and are suggestive of the statistical nature of the charged particle number density fluctuations in the two dimensional phase space. The absence of self similar and multifractal behaviors of the particle generation in the modal is revealed.

The results provide a quantitative baseline for understanding the role of collective and non-collective effects in multiplicity fluctuations.

ACKNOWLEDGEMENTS

The authors gratefully acknowledge financial support for this work from the Dean Research Studies, University of Jammu, through the research grant "...", and from the Department of Science and Technology (DST), Government of India, via the project "Indian participation in ALICE experiment at CERN" sanctioned under order No. 3015/1/2021/Gen/R&D-I/13283. Fakhar Ul Haider acknowledges the University of Jammu for the Ph.D. scholarship. The authors also thank the CERN lxxplus computing grid for the computational resources used in this analysis.

-
- [1] V. N. Gribov and L. N. Lipatov. Deep inelastic e p scattering in perturbation theory. *Sov. J. Nucl. Phys.*, 15:438–450, 1972.
 - [2] Steven Weinberg. *The First Three Minutes. A Modern View of the Origin of the Universe.* hhh, 1977.
 - [3] D. P. Barber et al. Discovery of Three Jet Events and a Test of Quantum Chromodynamics at PETRA Energies. *Phys. Rev. Lett.*, 43:830, 1979.
 - [4] Edward V. Shuryak. Quark-Gluon Plasma and Hadronic Production of Leptons, Photons and Psions. *Phys. Lett. B*, 78:150, 1978.
 - [5] T. Niida and Y. Miake. Signatures of QGP at RHIC and the LHC. *AAPPS Bull.*, 31(1):12, 2021.
 - [6] S. S. Adler et al. J / psi production in Au Au collisions at $s_{NN}^{1/2} = 200$ -GeV at the Relativistic Heavy Ion Collider. *Phys. Rev. C*, 69:014901, 2004.
 - [7] Lyndon Evans and Philip Bryant. Lhc machine. *Journal of Instrumentation*, 3(08):S08001, aug 2008.
 - [8] Gordon Baym and Henning Heiselberg. Event-by-event fluctuations in ultrarelativistic heavy ion collisions. *Phys. Lett. B*, 469:7–11, 1999.
 - [9] V. Koch, M. Bleicher, and S. Jeon. Event-by-event fluctuations and the QGP. *Nucl. Phys. A*, 698:261–268, 2002.
 - [10] Michael Kliemant, Raghunath Sahoo, Tim Schuster, and Reinhard Stock. Global Properties of Nucleus-Nucleus Collisions. *Lect. Notes Phys.*, 785:23–103, 2010.
 - [11] Misha A. Stephanov, K. Rajagopal, and Edward V. Shuryak. Event-by-event fluctuations in heavy ion collisions and the QCD critical point. *Phys. Rev. D*, 60:114028, 1999.
 - [12] Rudolph C. Hwa and C. B. Yang. Local Multiplicity Fluctuations as a Signature of Critical Hadronization at LHC. *Phys. Rev. C*, 85:044914, 2012.
 - [13] B. Bambah, J. Fingberg, and H. Satz. The Onset of Intermittent Behavior in the Ising Model. *Nucl. Phys. B*, 332:629–640, 1990.
 - [14] Helmut Satz. Intermittency and Critical Behavior. *Nucl. Phys. B*, 326:613–618, 1989.
 - [15] W. Braunschweig et al. Study of Intermittency in Electron - Positron Annihilation Into Hadrons. *Phys. Lett. B*, 231:548–556, 1989.
 - [16] Edward K. G. Sarkisyan, Aditya Nath Mishra, Raghunath Sahoo, and Alexander S. Sakharov. Multi-hadron production dynamics exploring the energy balance in hadronic and nuclear collisions. *Phys. Rev. D*, 93:054046, 2016. [Addendum: *Phys.Rev.D* 93, 079904 (2016)].

- [17] Nicolas Borghini. Multiparticle correlations from momentum conservation. *Eur. Phys. J. C*, 30:381–385, 2003.
- [18] Rudolph C. Hwa and M. T. Nazirov. Intermittency in second order phase transition. *Phys. Rev. Lett.*, 69:741–744, 1992.
- [19] Torbjörn Sjöstrand, Stefan Ask, Jesper R. Christiansen, Richard Corke, Nishita Desai, Philip Ilten, Stephen Mrenna, Stefan Prestel, Christine O. Rasmussen, and Peter Z. Skands. An introduction to PYTHIA 8.2. *Comput. Phys. Commun.*, 191:159–177, 2015.
- [20] Klaus Werner. EPOS4: New theoretical concepts for modeling proton-proton and ion-ion scattering at very high energies. *xxx*, 10 2024.
- [21] Torbjorn Sjostrand and Maria van Zijl. A Multiple Interaction Model for the Event Structure in Hadron Collisions. *Phys. Rev. D*, 36:2019, 1987.
- [22] Jesper R. Christiansen and Torbjörn Sjöstrand. Weak gauge boson radiation in parton showers. *Journal of High Energy Physics*, 2014(4), April 2014.
- [23] Christian Bierlich, Gösta Gustafson, Leif Lönnblad, and Harsh Shah. The angantyr model for heavy-ion collisions in pythia8. *Journal of High Energy Physics*, 2018(10), October 2018.
- [24] R. J. Glauber. Cross-sections in deuterium at high-energies. *Phys. Rev.*, 100:242–248, 1955.
- [25] Michael L. Miller, Klaus Reygers, Stephen J. Sanders, and Peter Steinberg. Glauber modeling in high-energy nuclear collisions. *Annual Review of Nuclear and Particle Science*, 57(1):205–243, November 2007.
- [26] Neelkamal Mallick, Sushanta Tripathy, Aditya Nath Mishra, Suman Deb, and Raghunath Sahoo. Estimation of Impact Parameter and Transverse Sphericity in heavy-ion collisions at the LHC energies using Machine Learning. *Phys. Rev. D*, 103(9):094031, 2021.
- [27] B. Ivanyi, Z. Schram, K. Sailer, and G. Soff. Nucleus-nucleus collisions in the dynamical string model. *Phys. Rev. C*, 61:024908, 2000.
- [28] Hong Pi. An Event generator for interactions between hadrons and nuclei: FRITIOF version 7.0. *Comput. Phys. Commun.*, 71:173–192, 1992.
- [29] K. Werner and B. Guiot. Perturbative QCD concerning light and heavy flavor in the EPOS4 framework. *Phys. Rev. C*, 108(3):034904, 2023.
- [30] K. Werner. Parallel scattering, saturation, and generalized abramovskii-gribov-kancheli (agk) theorem in the epos4 framework, with applications for heavy-ion collisions at $\sqrt{s_{NN}}$ of 5.02 tev and 200 gev, 2024.
- [31] Klaus Werner. Revealing a deep connection between factorization and saturation: New insight into modeling high-energy proton-proton and nucleus-nucleus scattering in the EPOS4 framework. *Phys. Rev. C*, 108(6):064903, 2023.
- [32] Jaroslav Adam et al. Centrality dependence of the pseudorapidity density distribution for charged particles in Pb-Pb collisions at $\sqrt{s_{NN}} = 5.02$ TeV. *Phys. Lett. B*, 772:567–577, 2017.
- [33] Jaroslav Adam et al. Centrality Dependence of the Charged-Particle Multiplicity Density at Midrapidity in Pb-Pb Collisions at $\sqrt{s_{NN}} = 5.02$ TeV. *Phys. Rev. Lett.*, 116(22):222302, 2016.
- [34] M. Bleicher et al. Relativistic hadron hadron collisions in the ultrarelativistic quantum molecular dynamics model. *J. Phys. G*, 25:1859–1896, 1999.
- [35] Michael L. Miller, Klaus Reygers, Stephen J. Sanders, and Peter Steinberg. Glauber modeling in high energy nuclear collisions. *Ann. Rev. Nucl. Part. Sci.*, 57:205–243, 2007.
- [36] A. Bialas and Robert B. Peschanski. Moments of Rapidity Distributions as a Measure of Short Range Fluctuations in High-Energy Collisions. *Nucl. Phys. B*, 273:703–718, 1986.
- [37] A. Bialas and Robert B. Peschanski. Intermittency in Multiparticle Production at High-Energy. *Nucl. Phys. B*, 308:857–867, 1988.
- [38] E. K. Sarkisian, L. K. Gelovani, and G. G. Taran. Fractality in central collisions of C-12 nuclei with Ne and Cu nuclei at 4.5-A/GeV/c. *Phys. Atom. Nucl.*, 56:832–840, 1993.
- [39] E. A. De Wolf, I. M. Dremin, and W. Kittel. Scaling laws for density correlations and fluctuations in multiparticle dynamics. *Phys. Rept.*, 270:1–141, 1996.
- [40] A. Kamal, N. Ahmad, and M. M. Khan. Study of Anomalous Fractal Dimensions and Scaling Exponent in Ginzburg–Landau Phase Transition in 14.5 A\,GeV/c ^{28}Si –AgBr Interactions. *Acta Phys. Polon. B*, 46(8):1549, 2015.
- [41] E. K. Sarkisian, L. K. Gelovani, and G. G. Taran. Fractality and fluctuations in charged particle pseudorapidity distributions in central C (Ne, Cu) collisions at 4.5-A/GeV/c. *Phys. Lett. B*, 302:331–335, 1993.